From runoff to rainfall: inverse rainfall-runoff modelling in a high temporal resolution

M. Herrnegger[1], H.P. Nachtnebel[1] and K. Schulz[1]

[1] {Institute of Water Management, Hydrology and Hydraulic Engineering, University of Natural Resources and Life Sciences, Vienna, Austria}

Correspondence to: Mathew Herrnegger (mathew.herrnegger@boku.ac.at)

Abstract

This paper presents a novel technique to calculate mean areal rainfall in a high temporal resolution of 60-min on the basis of an inverse conceptual rainfall-runoff model and runoff observations.

Rainfall exhibits a large spatio-temporal variability, especially in complex alpine terrain. Additionally, the density of the monitoring network in mountainous regions is low and measurements are subjected to major errors, which lead to significant uncertainties in areal rainfall estimates. The most reliable hydrological information available refers to runoff, which in the presented work is used as input for an inverted rainfall-runoff model. Thereby a conceptual, HBV-type model is embedded in a root finding algorithm. For every time step a rainfall value is determined, which results in a simulated runoff value that corresponds to the observation. The inverse model, also evaluating different model parameter sets, is applied to the Schliefau and Krems catchments, situated in the northern Austrian Alpine foothills. Generally, no substantial differences between the catchments are found. Compared to station observations in the proximity of the catchments, the inverse rainfall sums and time series have a similar goodness of fit, as the independent INCA rainfall analysis of Austrian Central Institute for Meteorology and Geodynamics (ZAMG). The application of the inverse model is a promising approach to obtain improved estimates of mean areal rainfall. These can be used to enhance interpolated rainfall fields, e.g. for the estimation of rainfall correction factors, the parameterisation of elevation dependency or the application in real-time flood forecasting systems. The application is limited to (smaller) catchments, which can be represented with a lumped model setup and to the estimation of liquid rainfall.

1 Introduction

The motivation for the concept presented in this paper comes from practical hydrological problems. Some years back we set up rainfall-runoff models for different alpine rivers (e.g. Stanzel et al., 2008; Nachtnebel et al., 2009a, 2009b, 2010a or 2010b). In the course of these projects, we were confronted with massive errors in the precipitation input fields. This is a known problem, especially in alpine environments. Although the temporal dynamics in the runoff simulations were captured quite well, significant mass balance errors between observed and simulated runoff were found. It could be excluded, that erroneous evapotranspiration calculations were biasing the results (Herrnegger et al., 2012). In the HYDROCAST project (Bica et al., 2011) we tested different precipitation interpolation and parameterisation schemes by using the ensemble of generated inputs for driving a rainfall-runoff model and comparing the simulated runoff time series with observations. In essence, the results showed, that no significant improvements could be made in the runoff simulations and that the information on the precipitation fields is strongly determined and limited by the available station time series. The only additional information available concerning the precipitation of a catchment is the runoff observation. The main aim is therefore to present a proof-of-concept for the inversion of a conceptual rainfall runoff model. That is to show, that it is possible to use a widely applied model concept to calculate mean areal rainfall from runoff observations.

Areal or catchment rainfall estimates are fundamental, as they represent an essential input for modelling hydrological systems. They are however subject to manifold uncertainties, since it is not possible to observe the mean catchment rainfall itself (Sugawara, 1992; Valéry et al., 2009). Catchment rainfall values are therefore generally estimated by interpolation of point measurements, sometimes incorporating information on the spatial rainfall structure from remote sensing, e.g. radar (e.g. Haiden et al., 2011). Measurement, sample and model errors can be identified as sources of uncertainty. Point observations of rainfall, which are the basis for the calculation of mean areal rainfall values, are error inflicted (Sevruk, 1981, 1986; Goodison et al, 1998; Sevruk and Nespor, 1998; Seibert and Moren, 1999; Wood et al., 2000; Fekete et al., 2004). Occult precipitation forms like fog or dew are frequently ignored. Although not generally relevant, this precipitation form can be a significant contribution to the water budget of a catchment (Elias et al., 1993; Jacobs et al., 2006; Klemm and Wrzesinsky, 2007). The highest systematic measurement errors of over 50 % are found during snowfall in strong wind conditions. Other sources of systematic measurement errors and their magnitudes are listed in Table 1.

➔ Approximate location of Tab. 1

In complex terrain the rainfall process is characterised by a high temporal and spatial variability. Especially in these areas the density of the measurement network tends to be low, not capturing the high variability and leading to sample errors (Wood et al., 2000; Simoni et al., 2011; de Jong et al., 2002). Further uncertainties arise in the interpolation of catchment scale rainfall from point observations. Systematic and stochastic model errors of the regionalisation methods can be identified. Systematic model errors can arise during the regionalisation of rainfall in alpine areas, when e.g. the elevation dependency is not considered (Haiden and Pistotnik, 2009). Quantitative areal rainfall estimates from radar products are, although they contain precious information on the rainfall structure, still afflicted with significant uncertainties (Krajewski et al., 2010; Krajewski and Smith, 2002). A general magnitude of overall uncertainty, which arises during the generation of areal rainfall fields, is difficult to assess, as different factors, e.g. topography, network density or regionalisation method, play a role.

Errors in runoff measurements are far from negligible (Di Baldassarre and Montanari, 2009; McMillan et al., 2010; Pappenberger et al., 2006; Pelletier, 1987). When applying the rating-curve method for estimation of river discharge the uncertainties are a function of the quality of the rating curve and the water level measurements. The quality of the rating curve depends on (i) the quality and stability of the measured cross-section over time, (ii) the representativeness of the velocity measurements and (iii) the influence of steady and unsteady flow conditions. According to literature the overall uncertainty, at the 95 % confidence level, can vary in the range of 5% - 20% (Di Baldassarre and Montanari, 2009; Pelletier, 1987). Although it can be expected, that the measurement error will certainly be large during flood events due to its dynamic features, the errors are considerable lower compared to rainfall measurements and to the uncertainties introduced, when calculating mean areal rainfall. It must however be assumed, that transboundary flows and groundwater flows around the gauging station are negligible.

A classical application of hydrology, the problem of reproducing observed runoff with meteorological forcings as input through a formalised representation of reality, is a forward or direct problem. Two inverse problems can be identified with the forward problem (Groetsch, 1993):

1. Causation problem: Determination of input I (=cause), with given output O (=effect) and given model K, including model parameters θ (=process)

2. Model identification problem: Determination of model K, given input I and output O

The model identification problem can be divided into (i) the problem of identifying the model structure itself and (ii) the determination of model parameters that characterise the system (Tarantola, 2005). The focus in this contribution lies in solving the causation problem, i.e. in the determination of rainfall input from runoff, with a given model structure and parameters. In the following, the model, which calculates mean catchment rainfall values from runoff, will be called *inverse model*. The conventional model, which uses rainfall and potential evapotranspiration as input to calculate runoff, will be called *forward model*.

Runoff from a closed catchment is the integral of rainfall over a certain period, considering evapotranspiration losses and water storage characteristics within the catchment. Therefore, runoff observations can be used to derive information on rainfall. This has been done in several studies, e.g. Bica et al., 2011; Valéry et al., 2009, 2010; Ahrens et al., 2003; Jasper and Kaufmann, 2003; Kunstmann and Stadler, 2005 or Jasper et al., 2002. The common basis of these studies was to indirectly gain information on catchment rainfall by comparing simulated runoff results with observations. Hino and Hasabe (1981) fitted an AR (autoregressive) model to daily runoff data, while assuming rainfall to be white noise. By inverting the AR model they directly generated time series of rainfall from runoff. Vrugt et al. (2008) and Kuczera et al. (2006) derived rainfall multipliers or correction factors from stream flow with the DREAM- and BATEA-methods, these methods however being computationally intensive. In a well-received study, Kirchner (2009) analytically inverted a single-equation rainfall-runoff model to directly infer time series of catchment rainfall values from runoff. The Kirchner model (when deriving the storage-discharge relationship directly from runoff data) only has a single parameter and does not need rainfall as driving input for calibration. Rainfall data is however needed for the determination of rainless periods for the estimation of the sensitivity function. Krier et al. (2012) applied the model of Kirchner (2009) to 24 small and mesoscale catchments in Luxembourg to generate areal rainfall. No systematic differences in the quality of the rainfall estimates are found between different catchment sizes. In periods with higher soil moisture the rainfall simulations show a higher performance, which is explained by the fact, that wet catchments are more likely to react as simple dynamical systems. The parsimonious approach of Kirchner (2009) is however limited to catchments, where discharge is determined by the volume of water in a single storage and which can be characterized as simple first-order nonlinear dynamical systems. Also due to the larger number of model parameters describing several linked storages, accounting for a variety of different runoff components, HBV-type conceptual models offer higher degrees of freedom and flexibility in the calibration procedure. They can, in consequence, be applied to catchments with a wider range of runoff characteristics (Bergström, 1995; Kling et al., 2015; Kling, 2006; Perrin et al., 2001). Therefore, in this study, the conceptual rainfall-runoff model COSERO (Nachtnebel et al., 1993; Eder et al., 2005; Kling and Nachtnebel, 2009, Herrnegger et al., 2012; Kling et al., 2015, among others), which in its structure is similar to the HBV-model, is used as a basis for the inverse model. The COSERO model has been frequently applied in research studies, but also engineering projects (see Kling et al., 2015 for details).

This paper is organized as follows: Following this introduction the methods-section describes the conventional conceptual rainfall-runoff model (forward model) and the inverse model, including the preconditions and limitations of its application. The concept of virtual experiments to test the inverse model and to analyse the existence, uniqueness and stability of the inverse rainfall simulations are presented. Additionally, the setup of different simulation experiments, e.g. to evaluate the influence of differing calibration periods or possible runoff measurement errors on the simulations, are explained. The inverse model is applied to two headwater catchments in the foothills of the northern Austrian Alps, with differing hydro-climatic and physical conditions. The catchments and the data base, including the calibration periods for the simulation experiments, is presented. The runoff simulations of the forward model and the rainfall simulations of the inverse model are described in detail in the results and discussion section. Finally the paper ends with a summary and conclusions.

2 Methods

2.1 Forward model (Rainfall-runoff model)

In the state space formulated forward model, the unknown runoff Q_t is a function f of known variables rainfall input R_t, potential evapotranspiration ETp_t, system states S_{t-1} and a set of model parameters θ_i, whereas the index t denotes time:

$$Q_t = f(R_t, ETp_t, S_{t-1} \mid \theta_i) \tag{1}$$

The rainfall-runoff model is based on the COSERO model (see introduction for references), but has a simpler model structure. It includes an interception and soil module and three reservoirs for interflow, base flow and routing. The model structure is shown in Fig. 1, model parameters are summarized in Table 2 and fluxes and system states in Table 3.

➔ Approximate location of Fig. 1

➔ Approximate location of Tab. 2

➔ Approximate location of Tab. 3

The COSERO-model is formulated in a state space approach, with state transition functions

$$S_{\mathrm{t}} = f(S_{\mathrm{t-1}}, I_{\mathrm{t}} \mid \theta_{\mathrm{i}}) \qquad (2)$$

and output functions

$$O_{\mathrm{t}} = f(S_{\mathrm{t-1}}, I_{\mathrm{t}} \mid \theta_{\mathrm{i}}) \qquad (3)$$

with

I_t Input, e.g. rainfall

O_t Output, e.g. total runoff

S_t System states, e.g. water stored in soil module

θ_i Model parameters.

These functions have a time component, which is indicated by the index "t". So, the model state and the output at time t depend only and exclusively on the previous state S_{t-1}, the inputs I_t and parameters θ_i. The simplified model formulation can be found in the appendix.

2.2 Inverse model (Runoff-rainfall model)

In the inverse model the unknown rainfall R_t is a function of runoff Q_t, potential evapotranspiration ETp_t, system states S_{t-1} and a given set of model parameters θ_i, where again the index t denotes time:

$$\mathrm{R}_{\mathrm{t}} = f^{-1}(Q_{\mathrm{t}}, ETp_{\mathrm{t}}, S_{\mathrm{t-1}} \mid \theta_{\mathrm{i}}) \qquad (4)$$

Given ETp_t, S_{t-1} and θ_i, there is only one single input I_t, which results in an output O_t (eq. (3))! To calculate the inverse rainfall rate the forward model is therefore embedded in a search algorithm, to find, for every time step t, the rainfall rate R_t that best fits the observed runoff:

$$\mathrm{f}(\mathrm{R}_{\mathrm{t}}) = QSIM_{\mathrm{t}}(R_{\mathrm{t}}, ETp_{\mathrm{t}}, S_{\mathrm{t-1}} \mid \theta_{\mathrm{i}}) - QOBS_{t} \leq \varepsilon \tag{5}$$

with

$$\mathrm{R}_{\mathrm{t,min}} \leq \mathrm{R}_{\mathrm{t}} < \mathrm{R}_{\mathrm{t,max}} \tag{6}$$

The upper and lower brackets of rainfall ($R_{t,min}$ and $R_{t,max}$) is set to 0 and 50 mm/h. The value of the upper bound is an arbitrary value, but any reasonable bounds can be applied. $QSIM_t$ and $QOBS_t$ is the simulated and observed runoff. ε denotes a small value, which is ideally zero.

Solving eq. (5), which reflects the objective function used in the search algorithm, is basically a root finding problem. Different root finding algorithms were tested, with the Van Wijngaarden–Dekker–Brent Method (Brent, 1973; Press et al., 1992) being the method of choice, as this method exhibited the fastest results. The Brents method combines root bracketing, bisection and inverse quadratic interpolation to converge from the neighbourhood of a zero crossing and will always converge, as long as the function can be evaluated within the initial defined interval (in our case $R_{t,min}$ and $R_{t,max}$) known to contain a root (Press et al., 1992). The iteration progress for one model time step is illustrated in Fig. 2. The left y-axis shows the objective function values, the right y-axis (in logarithmic scale) the associated rainfall values estimated during the iteration procedure.

➔ Approximate location of Fig. 2

The state space approach of the model is a first order Markov process: The system states S_t and outputs O_t of the calculation time step depend only on the preceding states S_{t-1} and some inputs I_t and not on the sequences of system states, that preceded it, e.g. S_{t-2}, S_{t-3}, ..., S_{t-n} (see eq. (2) and eq. (3)). All information of the sequence of the preceding inputs (I_{t-1}, I_{t-2}, ..., I_{t-n}) is implicitly included in the last relevant system state S_{t-1}. No hysteretic effects are considered in the model and it does not include a parameter, which introduces a lag effect between inputs and outputs.

Given the model structure, parameters and potential evapotranspiration as input, the inverse rainfall and resulting runoff are solely a function of the initial cold system states. The influence of the initial cold system states on the inverse rainfall calculation are analysed in the results section.

The determined rainfall value R_t represents the "best" simulated rainfall of the catchment and is also used as input into the forward model to simulate runoff. Therefore, for every time step the inverse model simulates a rainfall and corresponding runoff value and also resulting system states. The simulated runoff value should ideally be identical to the observed value. This is however not always the case, as will be shown later.

A more elegant method to calculate rainfall from runoff is by analytically inverting the equations of a given model, i.e. bringing the rainfall term onto the right side of the equation (Herrnegger, 2013). This is principally possible, but has some disadvantages. The model structure, which was used in Herrnegger (2013) and which can be inverted analytically, differs from the model presented here. It does not include interception and routing. Additionally the inversion is not possible in certain periods, since the discontinuities introduced by threshold values lead to non-inversibility in the analytical solution (Herrnegger, 2013). For the forward model used here, the differential equations of the linear reservoirs are solved analytically. An internal time step discretization is included in the model code to guarantee, that the transition between system states above and below the threshold value are solved exactly. This is not possible in the analytical solution.

2.2.1 Preconditions and limitations of the application of the inverse model

It must be assumed that runoff from the catchment passes through the measurement cross-section of the gauging station and that subsurface and transboundary flows are negligible. It does not make sense to apply the inverse model to leaky catchments or catchments, where a significant part of the runoff is not observed at the gauging site. Even with a given quantification of the leakage process, the application of a hydrological model would lead to an additional uncertainty difficult to quantify. This is however not necessarily a limitation of the inverse model. Also the application of a forward hydrological model, which needs to be calibrated against runoff observations, will fail or will result in wrong estimates of water balance components.

The inverse model is based on a lumped model setup and the resulting inverse rainfall value corresponds to the mean areal rainfall. Applying a spatially distributed model is not possible, since the origin of outputs of different zones or cells of a distributed model setup cannot be reproduced by the inverse model in a deterministic way without additional assumptions. The information of origin gets lost as soon as cell values are summed and routed to a catchment runoff value. It is however conceivable to spatially disaggregate the mean areal rainfall from the inverse model using additional information, e.g. assuming an elevation dependency of rainfall.

Solid precipitation is accumulated without any direct signal on the hydrograph. It is therefore impossible to use the inverse model to estimate solid precipitation. The inverse model can therefore only be used to calculate rainfall in snow-free catchments, or, as in our case, periods, in which runoff is not influenced by snow melt (i.e. summer months). However, in rainless periods, where it is clear, that snow melt is dominating runoff (e.g. in spring), the inverse model can be used to quantify snow melt rates from a catchment.

The applicability of the inverse model is limited to catchments, which are representable with a lumped model setup and the proposed model structure. If a catchment is too large, one will generally have problems modelling that system with a lumped model setup. Not necessarily because of neglecting spatial heterogeneity in the model parameters (although this may also be an issue) or ignoring a lag between the rainfall and runoff signal, but simply because the lumped rainfall input used is "wrong" and is not representable for the whole catchment. If it only rains in the headwaters of large catchment, the lumped input into the forward model for this time step or rainfall event will be much lower, since it will be spatially aggregated. This input is simply not applicable to the whole catchment and the simulations will show deficits. In this case, an inversion will be highly flawed.

It is also clear, that catchments, independent of size, exist, where the application of this particular model structure will fail (e.g. flatland catchments dominated by groundwater). If hydro-meteorological conditions of the catchment change or are different from the calibration period and the forward model (e.g. due to poor parameter estimation, inadequate model structure, wrong representation of the real world prototype etc.) is not able to capture these changes, then again the calculation of rainfall from runoff will fail (as they do for the forward case).

However, being able to fit the forward model to observed runoff data and as long as the forward model is able to represent the catchment responses to rainfall, an inversion will be possible.

2.3 Simulation setups

2.3.1 Virtual experiments

In a first step the inverse model is evaluated and tested with virtual experiments, in which the preconditions of existence, uniqueness and stability of the inverse rainfall values are evaluated. Runoff simulations are performed with the forward model driven by observed rainfall as input. The simulated runoff time series of the forward models are then used as input into the inverse model, with the aim to reproduce the observed rainfall. Simulated runoff from the forward model is dependent on the model parameters. Therefore, to test the inversion procedure for the whole parameter range, synthetic hydrographs are produced with Monte Carlo simulations. 20 000 different parameter combinations are chosen randomly from the parameter space, with the same number of model runs to evaluate the inverse model. The sampled parameters and associated range are shown in Table 2. The schematic setup of the virtual experiment and the evaluation of the inverse model is shown in Fig. 3. Note, that the setup and the evaluation is performed for every individual Monte Carlo run, as the simulated runoff from the forward model varies, depending on selected model parameters.

➔ Approximate location of Fig. 3

The virtual experiments enable a rigorous evaluation of the inverse calculations, neglecting uncertainties concerning measurement errors in runoff, model structure or model parameters. All system states and fluxes of the forward model are perfectly known at every time step. This information is used to evaluate the inverse models. Only after a successful evaluation of the inverse model with the virtual experiments, can observations of runoff be used as input into the inverse models.

2.3.2 Model calibration and simulations experiments with observed data

The application of the inverse model is based on the assumption that the forward model can represent the catchment responses to rainfall, but needs to be calibrated against runoff observations. Depending on the calibration setup, different model parameters will be estimated. The calibration setup and in consequence model parameters (for a given model structure) can depend on (i) the calibration period and length and (ii) the driving input used. The inverse rainfall is also a function of the observed runoff, which may also exhibit possible measurement errors. Finally, the initial conditions of the system states at the beginning of the simulations also influence the results of the forward, but also inverse model. To evaluate these influences, i.e. different model parameters due to different calibration periods and lengths, different runoff observations, different parameter optimisation data basis and different initial conditions, several simulation experiments are performed. An overview table of the simulation experiments can be found in section 3.3 (Table 5) after the presentation of the available data.

The model structure applied includes 12 parameters, of which 10 have to be calibrated. Two parameters (INTMAX and ETVEGCOR) are estimated a priori (see Table 2). The simulation experiments do not allow a systematic analysis of parameter uncertainty or the assessment of equifinality. This is not the aim of this paper. The simulation experiments however enable a first assessment of the robustness of the results. That is to show the forward and inverse model performance, when the conditions are different from the conditions the model has been calibrated against or if different driving inputs are used.

In a first step 3 different periods are used for calibration of the model parameters. In a further simulation experiment, the runoff observation is increased by a constant offset of 10% to evaluate the influence of possible streamflow errors on the simulations and the inverse rainfall. A fifth experiment is performed, in which a differing rainfall realisation is used as driving input for model calibration, in order to test the conditioning of the model parameters and in consequence the simulations to the driving input. Given the model structure, the inverse rainfall is a function of observed runoff, potential evapotranspiration, system states and model parameters (eq. (4)). Extending eq. (4) explicitly with all relevant system states leads to

$$\mathrm{R_t} = f^{-1}(Q_{\mathrm{t}}, ETp_{\mathrm{t}}, BWI_{\mathrm{t-1}}, BW1_{\mathrm{t-1}}, BW2_{\mathrm{t-1}}, BW3_{\mathrm{t-1}}, BW4_{\mathrm{t-1}} \mid \theta_{\mathrm{i}}) \qquad (7)$$

The forward and inverse models are run as a continuous simulation in time. The preceding system states are therefore an integral part of the simulation and are determined intrinsically within the simulation. However, the initial system states at the beginning of the simulation period (cold states) will influence the results of the simulation, but should, after an adequate spin-up time, not influence the runoff but also inverse rainfall simulations. Therefore, a sixth experiment was set up, in which 3 different cold start scenarios are defined:

- Reference scenario
- Dry system states scenario

- Wet system states scenario

For the reference scenario the system states from the continuous simulation were used. For the cold states in the dry scenario the states from the reference scenario where reduced by the factor 0.5 and increased by the factor 1.5 for the wet scenario.

Generally only June, July, August and September are used, since it can be guaranteed, that no snow melt influences runoff in these months (see section 2.2.1). Parameter calibration in the simulation experiments is performed for the forward model, using the Shuffled Complex Evolution Algorithm (Duan et al., 1992). As an optimisation criterion the widely used Nash-Sutcliffe-Efficiency (NSE, Nash and Sutcliffe, 1970) was chosen.

3 Materials

3.1 Study areas

The inverse model is applied to two catchments with different size, geology and land use located at the foothills of the Northern Alps. The Schliefau catchment is located about 110 km south-west of the Austrian capital of Vienna and covers an area of 17.9 km² with a mean elevation of 608 m.a.s.l.. About 55% of the area is covered by grassland and meadows, 40% by coniferous forest and 5% by mixed forest. The underlying geology is dominated by marl and sandstone. The Krems catchment is located about 170 km south-west of the Austrian capital of Vienna and covers an area of 38.4 km² with a mean elevation of 598 m.a.s.l.. The topography is more heterogeneous, with an elevation range of 413 to 1511 m.a.s.l., compared to 390 to 818 m.a.s.l. in the Schliefau catchment. Approximately 46% of the area is covered by grassland and meadows, 48 % by mixed forest, 4 % by settlements and 2 % by coniferous forest. On a long term basis, in both catchments, the highest runoff can be expected during snow melt in spring, the lowest runoff in summer and autumn until October. Fig. 4 shows a map of the catchments and Table 4 summarizes important characteristics of the study areas.

➔ Approximate location of Fig.4

➔ Approximate location of Tab.4

3.2 Meteorological database

Generally, two different rainfall time series are used. Ground observations of rainfall are available from the station St. Leonhard im Walde (Schliefau catchment) and Kirchdorf

(Krems catchment), both located in the proximity of the catchments (Fig. 4). Additionally, areal rainfall data from the INCA system (Integrated Nowcasting through Comprehensive Analysis; Haiden et al., 2011) is used. INCA is the operational nowcasting and analysis application developed and run by the Central Institute for Meteorology and Geodynamics of Austria (ZAMG), which is also used for the majority of real-time flood forecasting systems in Austria (Stanzel et al., 2008). For the presented study analysis fields derived from observations, but no nowcasting fields, are used. Rainfall in INCA is determined by a nonlinear spatial interpolation of rain-gauge values, in which the radar field is used as a spatial structure function. In addition an elevation correction is applied (Haiden and Pistotnik, 2009). The stations used for the interpolation of the INCA-rainfall fields are shown as triangles in Fig. 4. Note, that the stations St. Leonhard im Walde and Kirchdorf are not included in the INCA analysis, since they are operated by a different institution. The rainfall fields from the INCA system cover the test basins in a spatial resolution of 1 km^2. From the spatial data set mean catchment rainfall values are obtained by calculating area-weighted means from the intersecting grid cells.

Potential evapotranspiration input is calculated with a temperature and potential radiation method (Hargreaves and Samani, 1982).

3.3 Simulation periods

Runoff and rainfall data is available for the period 2006 to 2009 in a temporal resolution of 60 minutes, which is also the modelling time step. The virtual experiments are performed for a period of 4.5 months (15.5.2006 – 30.09.2006) resulting in 3336 time steps being evaluated. As described in section 2.3.2 different model calibration and simulation experiments are performed. An overview of these experiments is given in Table 5.

➔ Approximate location of Tab.5

4 Results and discussions

4.1 Virtual experiments

In the virtual experiments it could be shown, that the precondition of existence, uniqueness and stability of the inverse model results is given. Using all 20 000 simulated hydrographs from the Monte Carlo runs, where the parameters were varied stochastically, the observed rainfall time series could be identically reproduced by the inverse model. Apart from the rainfall also all fluxes and system states where identical in the forward and inverse model runs. The comprehensive results from the virtual experiments are documented in Herrnegger (2013). Fig. 5 shows as an example of a virtual experiment the identical (i) observed rainfall and simulated inverse rainfall and (ii) system state of soil water content from the forward and inverse model. Station data from the Schliefau catchment with model parameters of Exp3 (see Table 5) were used as driving input in the forward model and the resulting runoff simulation in succession as input into the inverse model.

➔ Approximate location of Fig.5

4.2 Forward model: Parameter calibration and validation of the different simulation experiments

A precondition for the application of the inverse model is that the observed runoff characteristics of the catchment are reproduced reasonably by the forward model, since these parameters are also used in the inverse model. The following section therefore presents the runoff simulations of the forward model, based on the different simulation experiments Exp1 to Exp5.

The model performance for the period 2006 to 2009 of the forward model, expressed by Nash-Sutcliffe-Efficiency (NSE) and the mean bias between simulated and observed runoff in percent of observed runoff is shown in Table 6. As mentioned before, only the months June, July, August and September of the single years are used.

➔ Approximate location of Tab.6

For Exp1 to Exp3, the NSE-values for the period 2006 to 2009 show, that the overall model performance is fairly stable and comparable, independent of the calibration length. The NSE-values are larger than 0.82, with the exception of Exp1 in the Krems catchment. Although the calibration lengths and periods in Exp2 and Exp3 differ, identical model parameters were found for the Krems catchment in the optimisation for both simulation experiments. As a consequence the model performance is identical in these two experiments for the period 2006 to 2009. The mean bias does not show a clear pattern and seems to be independent from the calibration period and length. In the Schliefau catchment observed runoff is overestimated by 7.8 to 0.9 % and underestimated by -1.4 to -4.8% in the Krems catchment for the period 2006-2009, depending on the simulation Exp1 to Exp3. Overall the calculated bias between observed and simulated runoff is in reasonable bounds.

In Exp4 the observed runoff is increased by 10%, mainly to evaluate the influence of possible streamflow errors on the simulations and the inverse rainfall. The same calibration periods were used as in Exp3, with station observations as driving input into the model. The NSE of Exp4 is comparable to Exp1, Exp2 and Exp3. The mean bias in Exp4 however becomes larger. The observed runoff is now also underestimated in the Schliefau catchment, what is not surprising, since observed runoff was increased. The mean bias in Exp4 for the Krems catchment is also larger, compared to Exp1 to Exp3. This is also explained by the increased observed runoff.

In Exp5 INCA rainfall data is used as driving input for the simulations. The main intention of Exp5 is to evaluate the influence of a different rainfall input on the calibration of the model parameters and in consequence also on the inverse rainfall. For both catchments, the NSE values of the forward model are significantly lower, also compared to Exp3, which has the same calibration and validation periods. Although INCA uses a complex interpolation scheme, also incorporating radar data (Haiden et al., 2011), it seems that the data set has deficits representing catchment rainfall compared to the station observations in the proximity of the catchments. This can be explained by the larger distance of about 10 to 35 km of the INCA stations from the catchment (see Fig. 4). Note, that the ground observations in the proximity of the catchments are not used in in the interpolation process for the INCA-rainfall fields, as they belong to a monitoring network operated by a different institution.

Fig. 6 shows the NSE-values of the forward model for the calibration periods of every simulation experiment versus single years performance for the 2 study areas.

➔ Approximate location of Fig.6

For Exp1 a significant larger spread in the model performance within the single years is evident. In Exp1 only 2006 was used for calibration. As a consequence, especially for the Krems catchment, the model performance is lower in the years 2007 to 2009, compared to Exp2 and Exp3. In the short calibration period of 2006 the model parameters are overfitted to the observations. If the conditions in the catchment are different from the calibration period, the model performance can be expected to deteriorate, as has been shown before (e.g. Kling, 2015; Seibert, 2003) and explains the findings. For Exp2 to Exp4 the model performance is however stable for the single years, also for 2009, which was not used for calibration in any simulation experiment. In contrary to the Krems area, a large spread in the model performance of the single years for Exp5 is visible in the Schliefau catchment. The reason is not clear and may be explained by changing availability of station data for the INCA rainfall in the single years. We can however not verify this hypothesis, since we do not have access to the data sets. In the Schliefau catchment low NSE values are calculated for the year 2008 for all simulation experiments. In the beginning of June a flood was observed (Fig. 7), which is not simulated in the model runs and explains the lower NSE values in this year. Excluding this event in the performance calculations would, result in a significantly higher NSE of 0.84 for Exp1 for the year 2008, compared to 0.63 when the flood event is included in the calculation.

Fig. 7 (Schliefau) and Fig. 8 (Krems) exemplarily show the runoff simulations based on the results of Exp2. For both catchments, the dynamics and variability of the runoff observations are mostly reproduced in a satisfactory manner. However, a tendency is visible, that larger floods are underestimated in the simulations.

➔ Approximate location of Fig.7

➔ Approximate location of Fig.8

All simulations are performed with a lumped model setup. Consequently heterogeneity in geology and land use within the catchment are not considered in the parameter estimation. Also taking this into consideration, it can be concluded that the general responses of the catchment to rainfall input are captured appropriately by the forward model. Only for Exp1 with the very short calibration period, a larger spread in the model performance is evident in independent years. It is therefore justified to calculate areal rainfall from runoff using the inverted forward model, including the optimised parameters.

4.3 Inverse model

For the evaluation of the simulated rainfall from the inverse model (PInv) we will compare the calculated values with observed station data (PObs) of St. Leonhard (Schliefau catchment) and Kirchdorf (Krems catchment) and the rainfall values from the INCA-system (PInca). In the following cumulative rainfall sums and the correlation and bias between simulated and observed rainfall are presented. Additionally the rainfall and runoff simulations of a flood event and the influence of cold system states on the simulations are shown.

4.3.1 Cumulative rainfall sums

Fig. 9 and 10 show the cumulative curves of the observed rainfall (PObs), INCA rainfall (PInca) and the inverse rainfall (PInv) of the simulation experiments Exp1 to Exp5 for the Schliefau and Krems catchment. Additionally the cumulative observed runoff (Qobs) is shown as a dashed line. Note that for the Krems catchment (Fig. 10) the rainfall curves of Exp2 and Exp3 are identical, since the model parameters are also identical in these simulation experiments.

➔ Approximate location of Fig.9

➔ Approximate location of Fig.10

The cumulative sums of the inverse rainfall and the observation based rainfall realisations PObs and PInca mostly show very similar temporal dynamics. Although large deviations are sometimes evident for both catchments, the deviations of the cumulative curves of PInca and the different inverse rainfalls (PInv) from the cumulative curves of the ground observation (PObs) are mostly of similar magnitude.

The inverse rainfall curves of Exp1 to Exp5 of the two catchments do not exhibit substantial differences, although different calibration periods and setups were used. At the beginning of June 2008 a flood was observed in the Schliefau catchment, which was underestimated in the forward simulation, presumably due to inadequate representation of the storm event in the rainfall observations (see runoff simulation in Fig. 7, lower left). Larger rainfall intensities are therefore calculated by the inverse for this period, leading to the larger deviations between the cumulative sums of PObs and PInv of Exp1 to Exp5 as shown in Fig. 9 (lower left). In the Schliefau catchments larger differences between Exp1 to Exp5 occur in the year 2009 (Fig. 9, lower right). Here, in the second half of June, a period of strong rainfall is evident, which also led to a series of floods in the catchment (see also the hydrographs in Fig. 7). The rainfall sums originating from these high flows were calculated differently in the inverse models, depending on the simulation experiment. In consequence, the inverse rainfall curves differ from July onwards. In 2009, which was the wettest summer in both catchments, the highest inverse rainfall sums are found for Exp4. This is what could be expected, since the observed runoff was increased by 10% in this simulation experiment. However, in the other years Exp4 does not necessarily show the largest inverse rainfall sums. The optimised model parameters in Exp4, that control evapotranspiration, were limiting actual evapotranspiration from the model to fulfil the water balance, since PObs was not changed. In the second half of June 2009, during the flood events with low evapotranspiration, the higher runoff values used as input however show a clearer signal in the inverse rainfall sums.

The large difference between cumulative rainfall and runoff curves highlight the importance of actual evapotranspiration (ETa) in the catchments. For the Schliefau catchment the mean observed rainfall for the summer months of 2006-2009 is 678 mm. 266 mm are observed in the mean for runoff. Neglecting storage effects, a mean actual evapotranspiration of 412 mm can be calculated from the water balance. Over 60 % of rainfall are therefore lost to evapotranspiration. The mean actual evapotranspiration from the inverse model, depending on the simulation experiment, range from 352 mm to 362 mm, and are lower compared to the ETa calculated from the water balance. In the Krems catchment a mean runoff of 334 mm and rainfall of 600 mm, resulting in an actual evapotranspiration of 266 mm, is calculated. Although lower compared to Schliefau, nearly 45 % of rainfall are here lost to the atmosphere. The mean actual evapotranspiration from the inverse model, again depending on the simulation experiment, range from 276 mm to 310 mm. ETa from the model reflects the complex interplay and temporal dynamics of the system states of the different parts of the model. If the model would not capture ETa adequately, the cumulative rainfall curves would not follow the observations so closely.

On the basis of the different cumulative rainfall sums it can be concluded, that on a longer temporal basis, the inverse model is capable of simulating the catchment rainfall from runoff observations. The results from the different simulation experiments do not differ substantially and show close correspondence to the observed data, except for a single summer in the Schliefau catchment.

4.3.2 Correlation and bias between simulated and observed rainfall

The performance of the inverse model expressed by the correlation coefficient is used to measure the models ability to reproduce timing and shape of observed rainfall values. It is independent of a possible quantitative bias. In the introduction the difficulties involved in the quantitative measurement of rainfall were discussed. It can however be assumed that a qualitative measurement, e.g. if it rains or not, will be more reliable. Table 7 shows the correlation values for 2006 to 2009 between ground observations and the different inverse rainfall realisations (PObs – PInv) and ground observations and INCA rainfall (PObs – PInca) for different temporal aggregation lengths.

➔ Approximate location of Tab.7

For the 1h-sums, the lowest correlation values between PObs and PInv are found for the simulation results of Exp1 in both catchments. The highest correlation values are found for Exp2 in the Schliefau catchment and Exp2 to Exp4 in the Krems catchment. This agrees with the performance of the forward model presented in section 4.2.. The correlation of the 1h-sums between PObs and PInv is rather weak. However, the correlation between PObs and PInv is higher for all simulation experiments and 1h-sums compared to the correlation between PObs and PInca. This is interesting, since PInca is based on station rainfall observations and PInv is indirectly derived from runoff through simulations. With temporal aggregation the correlation values generally increase significantly for all combinations. Small differences or timing errors in the 1h-sums are eliminated with temporal aggregation. This is also the case in of the INCA data.

For Exp1 to Exp4, the model parameters used for the forward and inverse model were automatically calibrated using the ground observation PObs as input. It could therefore be concluded that the model parameters are conditioned by PObs and that in consequence the fairly good agreement between PObs and PInv originates from this conditioning. Based on this hypothesis, calibrating the model with INCA data should lead to a better agreement between the INCA data and the corresponding inverse rainfall and a deterioration of the correlation between station data and inverse rainfall. For Exp5, the forward model was therefore calibrated with INCA data and the resulting parameters set was then used to calculate the inverse rainfall. The correlation between PInca and PInv for Exp5 is however not higher, compared to the other simulation experiments and Exp3, which had the same calibration period. This excludes that the parameters are conditioned (at least for the rainfall simulations) by the input used for calibration. The correlations between PInca and PInv are generally very weak, with values ranging from 0.25 to 0.29 for the Schliefau and 0.39 to 0.445 for the Krems catchment. This corresponds to the performance of the forward model in Exp5. Here lower model performance of the forward model is found for the Schliefau catchment.

The correlation between PObs and PInv for the 1-h sums ranges between 0.48 and 0.55, but is higher, compared to the correlation between PObs and PInca. In contrast Kirchner (2009) shows correlation values between simulated and observed rainfall of 0.81 and 0.88 for his two sites. The Schliefau and Krems catchments differ substantially in size, hydrological characteristics, land use or geology. The NSE values of the runoff simulations in Kirchner (2009) are higher, compared to the values presented here for the forward model. As a consequence the better performance in the rainfall simulations may be explained with the fact, that the Kirchner (2009) model better reflects the catchment conditions leading to runoff.

For the 24-h sums we calculate a correlation of 0.87 to 0.92, depending on the catchment and simulation experiment. Here Kirchner (2009) shows correlation of 0.96 and 0.97. Krier et al. (2012) present correlations between simulated and observed rainfall of 0.81 to 0.98, with a mean value of 0.91 for a total of 24 catchments, however only on the basis of data of a single year. The correlation in our results is therefore in the range of other studies. Unfortunately Krier et al. (2012) do not present NSE values of the runoff simulations. It is therefore not possible to check the link between the performance of the forward model and rainfall simulations in their study.

Fig. 11 shows the correlation between PObs and PInv for the calibration periods of the simulation experiments Exp1 to Exp5 versus the correlation in single years for the two study areas. For the Schliefau catchment the largest spread in the correlation values of the single years is found for Exp1, which also corresponds to the performance of the runoff simulations of the forward model. For Exp2 to Exp5 a spread is also visible between the single years, but differences are smaller. For the years 2006, 2008 and 2009 the correlation values in the Krems catchment do not differ substantially. Here however the correlation for the year 2007 is very low, independent of the simulation experiment. This may be explained by the comparatively dry summer of 2007. Also in the Schliefau catchment the correlation values are mostly lower in 2007, compared to the other years.

➔ Approximate location of Fig.11

Tab. 8 summarizes the mean daily bias in mmd^{-1} for the summer months in 2006 to 2009 between different rainfall realisations. For the Schliefau catchment, the bias between PInv and PObs is mostly significantly higher, compared to the bias between PInca and PObs. Only Exp2, with a mean bias of 0.07 mmd^{-1}, is comparable to the bias between PInca and PObs of 0.02 mmd^{-1}. Exp2 also showed the highest performance in the runoff simulations concerning the NSE. In contrary, for the Krems catchment, the bias is lower between PInv and PObs for Exp1 to Exp3, compared to PInca-PObs. For Exp1 to Exp3 a mean bias of 0.14 mmd^{-1}

(Schliefau) and 0.36 mmd^{-1} (Krems) is calculated. As a comparison, Krier et al. (2014) published mean bias values between simulated and observed rainfall of -3.3 to 1.5 mmd^{-1} (mean -0.35 mmd^{-1}) for 24 catchments on the basis of a single year. From all simulation experiments, Exp4 shows the largest bias, which is explained by the fact, that runoff was increased in this experiment. Here the increased runoff clearly shows a signal in the inverse rainfall, in contrast to the correlation and cumulative sums shown above.

➔ Approximate location of Tab.8

4.3.3 Rainfall and runoff simulations for a flood event

Fig. 12 exemplarily illustrates the temporal development of the different rainfall realisations and runoff simulations for the highest flood event in the Krems catchment. Results from Exp3 are shown. Compared to PObs and PInca the inverse rainfall PInv exhibits higher variability and higher intensities. The higher variability and oscillating nature of the inverse rainfall is explainable with the reaction of the inverse model to small fluctuations in runoff observations: In case of rising runoff observations, rainfall will be estimated by the inverse model. If the observed runoff decreases and the simulated runoff of the inverse model is larger than observed runoff, no inverse rainfall will be calculated, leading to the visible oscillations. Fig. 12 (b) shows, that the forward model, driven with PObs as input, underestimates both flood peaks. The forward model, driven with the inverse rainfall, simulates the driven periods very well (Inverse QSim). However, especially the falling limb after the second flood peak on the 07.09.2007 is overestimated by the inverse model. In this period it is also visible, that in consequence no rainfall is calculated by the inverse model, since simulated runoff is higher than observed runoff.

➔ Approximate location of Fig.12

For a given time interval, the inverse model will yield an exact agreement between observed and simulated runoff, as long as there is a positive rainfall value R_t to solve eq. (5). This will be the case in periods of rising limbs of observed runoff (driven periods), as a rainfall value can be estimated, which raises the simulated runoff value to match observation. On the contrary, in periods of observed falling limbs (non-driven periods) the simulated runoff will solely be a function of the model structure, its parameters and the antecedent system states, as negative rainfall values are ruled out beforehand. This explains, why in periods, in which the simulated runoff is higher than the observed value, no rainfall is calculated by the inverse model.

4.3.4 Influence of cold system states on the inverse rainfall (Exp6)

To test the influence of cold states on the inverse rainfall simulations the simulation experiment Exp6 was performed. Three different cold states (Reference, dry and wet system states) were thereby defined (see section 2.3.2). Fig. 13 exemplarily shows the results of Exp6 for the Krems catchment.

➔ Approximate location of Fig.13

From the monthly rainfall sums of the different model runs it is evident, that the inverse rainfall calculations differ significantly at the beginning of the simulation. In the first month the reference scenario results in a monthly rainfall sum of 30 mm, the dry scenario in 111 mm and the wet scenario in only 9 mm. Generally the model will always strive towards an equilibrium in its system states, which are a function of the model structure and parameters. In the scenario "wet" a lot of water is stored in the states of the model at the beginning, with the result, that little inverse rainfall is calculated. In the dry scenario on the other hand a higher amount of rainfall is estimated, since less water is stored in the states at the beginning. With time, however, the different system states converge. In consequence also the inverse rainfall values converge and after 9 months no differences are evident.

As in forward models formulated in a state-space approach, it is evident that cold states have a noteworthy influence on the simulation results. After an adequate spin-up time the system states however converge, leading to deterministic and unique inverse rainfall estimates.

5 Summary and conclusions

A calibrated rainfall-runoff model (forward model) reflects the catchment processes leading to runoff generation. Thus, inverting the model, i.e. calculating rainfall from runoff, yields the temporally disintegrated rainfall. In this paper we applied a conceptual rainfall-runoff model, which is inverted in an iterative approach, to simulate catchment rainfall from observed runoff. The estimated inverse rainfall is compared with two different rainfall realisations: Apart of ground observations, areal rainfall fields of the INCA-system are used. The approach is applied to two study areas in Austria. Hourly data is available for the years 2006 to 2009. Only the months of June to September are used, as the inverse model can only be applied in periods, in which runoff is not influenced by snow melt (i.e. summer months).

In a first step, the forward model is calibrated against runoff observations. To evaluate the influences of (i) different model parameters due to different calibration periods and lengths, (ii) different runoff observations and (iii) different parameter optimisation data basis on the runoff and rainfall calculations, several simulation experiments are performed. Additionally the influence of different initial conditions on the rainfall simulations are evaluated.

The forward model mostly shows stable results in both catchments and reproduces the dynamics and variability of the catchment responses to rainfall in a satisfactory manner. Only the simulation experiment, in which a single summer was used for parameter calibration, shows a larger deterioration of the model performance in the independent years. The model parameters are then used for deriving catchment rainfall from runoff observations.

The cumulative rainfall curves of the rainfall realisations (ground observation (PObs), INCA (PInca) and inverse rainfall from the different simulation experiments (PInv)) are very similar, suggesting, that the inverse model is capable of representing the long-term quantitative rainfall conditions of the catchment. About 60 % (Schliefau) and 45% (Krems) of rainfall is lost to the atmosphere due to actual evapotranspiration (ETa). If the model would not capture ETa adequately, the cumulative rainfall curves would not follow the observations so closely.

The correlation between PInv and PObs, although rather low, is higher or of the same magnitude compared to the correlation between PObs and PInca, suggesting that the inverse model also reflects the timing of rainfall in equal quality of INCA. The correlation between PInv and PObs is mostly stable in the single years, independent of the simulation experiment. However, again for the simulation experiment with only a single summer for parameter calibration, a larger spread in the correlation for the single years is visible. An increase in observed runoff (Exp4) does not show negative effects on the inverse rainfall measured by the correlation coefficient. A larger bias between observed and modelled rainfall is however visible in Exp4. Generally, the simulation experiment with the highest performance in the runoff simulation also shows the highest correlation values in the rainfall simulations.

To test, if the inverse rainfall is conditioned by observed rainfall used as calibration input, additional model calibration is conducted using the INCA data as driving rainfall input for the forward model calibration. The simulation of inverse rainfall on the basis of this model parameters set show similar results as before, suggesting, that the inverse rainfall is not conditioned to the rainfall input used for model calibration.

Since the inverse model is formulated in a state-space approach additional simulations are performed with differing cold states at the beginning of the simulations. Here the results show, that the resulting inverse rainfall values converge to identical values after an adequate spin-up time.

Generally, the results do not differ substantially between the two test catchments. It can be concluded that the application of the inverse model is a feasible approach to estimate mean areal rainfall values. The mean areal rainfall values can be used to enhance interpolated rainfall fields, e.g. for the estimation of rainfall correction factors or the parameterisation of elevation dependency. With the inverse model, it is not possible to calculate solid rainfall. In rainless periods, where it is clear, that snow melt is dominating runoff (e.g. in spring), the inverse model can however be used to quantify the snow melt contribution.

The estimation of areal rainfall leading to extreme flood events is afflicted with major uncertainties. Here the inverse modelling approach can be used as an additional information source concerning the rainfall conditions during extreme events. In this context, it is conceivable to use the inverse model in real-time flood forecasting systems. Here two different applications of the inverse model are conceivable:

1. A frequent problem observed in real-time flood forecasting models with state space formulations is that the system states in the models are biased in such a way that the simulated and observed runoff differ systematically. Methods exist to cope with this problem and to update the system states (e.g. Liu et al, 2012; McLaughlin, 2002). The system states in the inverse model will, at least during driven periods, always guarantee, that the simulated runoff is identical to observations. This fact may be used as a basis for updating system states in the flood forecasting models.

2. At least in Austria, 2 different types of precipitation forecasts are used as input in flood or runoff forecasting models - nowcasting fields (used for forecasts of t=+1h to t=+6h) and fields from numerical weather forecasting models (used for t>+6h). The nowcasting fields strongly depend on the quality of station observations (t=0h), as they are the basis for extrapolation into the future (Haiden et al., 2011). By assimilating the inverse rainfall into the nowcasting system, i.e. to gain additional information on rainfall quantities, it is conceivable that the rainfall estimates of t=0h can be improved. An extrapolation of the improved rainfall fields could therefore improve the nowcasting fields and in consequence the runoff forecasts.

There are however several methodological issues to be solved, before an application in this context is possible. These include the spatial disaggregation of the inverse rainfall and system states in case the flood forecasting models are set up as distributed models or the limitation of the inverse model, when used to calculate rainfall, to snow-free periods. Additionally, the application presented here focused on headwater basins. In this context, the estimation of rainfall from intermediate catchments is also a future challenge.

In the presented work several different model parameter sets were used as a basis to calculate inverse rainfall. In further works the influences and uncertainties in the inverse rainfall, which arise from different model parameters should be analysed systematically. Additionally, a comparison of inverse rainfall estimates from a different model structure for the two catchments with our results would be of interest, in order to check the links between the performance of the forward model and the results obtained by the inversion method.

Appendix

The forward model is formulated as follows, considering parameters and variables in Table 2 and Table 3:

$$BWI_{t} = \max(\min(INTMAX, BWI_{t-1} + 0.5 * R_{t} - ETI_{t}), 0) = \max(\min(INTMAX, BWI_{t-1} + 0.5 * R_{t} - f(ETp_{t}, INTMAX)), 0) \tag{A1}$$

$$R\_Soil_{t} = 0.5 * R_{t} + \max(BWI_{t-1} + 0.5 * R_{t} - ETI_{t} - INTMAX, 0) \tag{A2}$$

$$\begin{aligned} BW0_{t} &= BW0_{t-1} + R\_Soil_{t} - ETG_{t} - Q1_{t} - Q2_{t} = \\ &BW0_{t-1} + R\_Soil_{t} - \min\left(\frac{BW0_{t-1}}{FKFAK * M}, 1\right) * (ETp_{t} - ETI_{t}) * ETVEGCOR - \\ &R\_Soil_{t} * \left(\frac{BW0_{t-1}}{M}\right)^{BETA} - f(PEX2) * BW0_{t-1} \end{aligned} \tag{A3}$$

$$\begin{aligned} BW2_{t} &= BW2_{t-1} + Q2_{t} - QAB2_{t} - QVS2_{t} = \\ &BW2_{t-1} + f(PEX2) * BW0_{t-1} - \alpha_{2} * \max(BW2_{t-1} - H2, 0) - \beta_{2} * BW2_{t-1} \end{aligned} \tag{A4}$$

$$BW3_{t} = BW3_{t-1} + QVS2_{t} - QAB3_{t} = BW3_{t-1} + \beta_{2} * BW2_{t-1} - \alpha_{3} * BW3_{t-1} \tag{A5}$$

$$\begin{aligned} BW4_{t} &= BW4_{t-1} + Q1_{t} + QAB2_{t} + QAB3_{t} - QSIM_{t} = \\ &BW4_{t-1} + R\_Soil_{t} * \left(\frac{BW0_{t-1}}{M}\right)^{BETA} + \alpha_{2} * \max(BW2_{t-1} - H2, 0) + \alpha_{3} * BW3_{t-1} - \alpha_{4} * BW4_{t-1} \end{aligned} \tag{A6}$$

with

$$\alpha_{i} = \frac{\Delta t}{TAB_{i}} \quad \text{and} \tag{A7}$$

$$\beta_{i} = \frac{\Delta t}{TVS_{i}} \tag{A8}$$

TAB_i / TVS_i = recession coefficients. Δt = modelling time step in units of hours. α and β vary with modelling time step and represent smoothing functions of the linear reservoirs

Eq. A1 to A8 are simplified representations of the model algorithm. Min/max operators, which, by introducing discontinuities, can lead to non-inversibility. Eq. A4 and A6 do not include a threshold function in the actual model code. The differential equations of the linear reservoirs are solved analytically. An internal time step discretization is included in the code, to guarantee, that the transition between system states above and below the threshold value is solved exactly. A3, representing the soil layer, does include a min() operator for estimating the ratio between actual and potential evapotranspiration as a function of soil water content. This is however not a limiting factor for the inversion, since this factor is a function of the preceding soil state $BW0_{t-1}$, which is known. Only 50% of rainfall is used as input into the interception storage BWI. By assuming that the other 50% are always throughfall, eq. A1 and A2 also doe not limit the inversion, since a continuous signal through the whole model cascade is guaranteed. The recession coefficient representing percolation processes in the soil layer exhibits a nonlinear characteristic and is calculated as a function of actual soil water content and a as a function of the form parameter PEX2 [-]. This model concept reflects the fact, that higher soil moisture levels lead to higher soil permeability values. These induce higher percolation rates which are reflected by lower recession coefficients.

References

Ahrens, B., Jasper, K., and Gurtz, J.: On ALADIN rainfall modeling and validation in an Alpine watershed, Ann. Geophys., 21, 627–637, doi:10.5194/angeo-21-627-2003, 2003.

Bergström, S.: The HBV model, in: Computer Models of Watershed Hydrology, edited by: Singh, V. P., Water Resources Publications, Highland Ranch, CO, USA, 443–476, 1995.

Bica, B., Herrnegger, M., Kann, A., and Nachtnebel, H. P.: HYDROCAST – Enhanced estimation of areal rainfall by combining a meteorological nowcasting system with a hydrological model, Final Report, Austrian Academy of Science, Vienna, doi:10.1553/hydrocast2011, 2011.

BMLFUW: Hydrological Atlas of Austria, 3rd Edn., Bundesministerium für Land- und Forstwirtschaft, Umwelt und Wasserwirtschaft, Wien, ISBN: 3-85437-250-7, 2007.

BMLFUW: Hydrographical yearbook of Austria, Abteilung VII 3 - Wasserhaushalt im Bundesministerium für Land und Forstwirtschaft, Umwelt und Wasserwirtschaft, Wien, 2009.

Brent, R.P.: Algorithms for Minimization without Derivatives, Prentice-Hall, Englewood Cliffs, NJ, 1973.

de Jong, C., List, F., and Ergenzinger, C.: Experimental hydrological analyses in the Dischma based on daily and seasonal evaporation, Nord. Hydrol. 33, 1–14, 2002.

Di Baldassarre G., and Montanari, A.: Uncertainty in river discharge observations: a quantitative analysis, Hydrol. Earth Syst. Sci., 13, 913-921, doi:10.5194/hess-13-913-2009, 2009.

Duan, Q., Sorooshian, S., and Gupta, V.K.: Effective and Efficient Global Optimization for Conceptual Rainfall-runoff Models, Water Resour. Res., 28, 1015-1031, 1992.

Eder, G., Fuchs, M., Nachtnebel, H.P., and Loibl, W.: Semi-distributed modelling of the monthly water balance in an alpine catchment, Hydrol. Process. 19, 2339–2360, 2005.

Elias, V., Tesar, M., and Buchtele, J.: Occult precipitation: sampling, chemical analysis and process modeling in the Sumava Mts. (Czech Republic) and in the Taunus Mts. (Germany), J. Hydrol., 166, 409–420, 1995.

Fekete, B.M., Vorosmarty, C.J., Roads, J.O., and Willmot, C.J.: Uncertainties in precipitation and their impacts on runoff estimates, J. Clim. 17, 294– 304, 2004.

Goodison, B.E., Louie, P.Y.T., and Yang, D.: WMO solid precipitation measurement intercomparison, Instruments and Observing Methods Rep. 67 (WMO/TD 872), World Meteorological Organization, Geneva, Switzerland, 318 pp, 1998.

Groetsch, C.: Inverse Problems in Mathematical Sciences, Vieweg Mathematics for Scientists and Engineers, Wiesbaden, 1993.

Haiden, T., and Pistotnik, G.: Intensity-dependent parameterization of elevation effects in precipitation analysis, Adv. Geosci., 20, 33–38, doi:10.5194/adgeo-20-33-2009, 2009.

Haiden, T., Kann, A., Wittman, C., Pistotnik, G., Bica, B., and Gruber, C.: The Integrated Nowcasting through Comprehensive Analysis (INCA) system and its validation over the Eastern Alpine region, Weather Forecast., 26, 166–183, doi:10.1175/2010WAF2222451.1, 2011.

Hargreaves, G.H., and Samani, Z.A.: Estimating potential evapotranspiration, J. Irr. Drain. Div-ASCE, 108, 225–230, 1982.

Herrnegger, M.: Zeitlich hochaufgelöste inverse Modellierung von Gebietsniederschlägen aus Abflussmessungen, PhD thesis, Institute of Water Management, Hydrology and Hydraulic Engineering, University of Natural Resources and Life Sciences, Vienna, Austria, 2013.

Herrnegger, M., Nachtnebel, H.P., and Haiden, T.: Evapotranspiration in high alpine catchments - an important part of the water balance!, Hydrol. Res. 43, 460-475, 2012.

Hino, M., and Hasabe, M.: Analysis of hydrologic characteristics from runoff data – a hydrologic inverse problem. J. Hydrol., 49, 287-313, 1981.

Jacobs, A.F.G., Heusinkveld, B.G., and Wichink Kruit, R.J.: Contribution of dew to the water budget of a grassland area in the Netherlands, Water Resour. Res., 42, W03415, doi:10.1029/2005WR004055, 2006.

Jasper, K. and Kaufmann, P.: Coupled runoff simulations as validation tools for atmospheric models at the regional scale. Q. J. Roy. Meteorol. Soc., 129, 673-692, 2007.

Jasper, K., Gurtz, J., and Lang, H.: Advanced flood forecasting in Alpine watersheds by coupling meteorological observations and forecasts with a distributed hydrological model, J. Hydrol., 267, 40-52, 2002.

Kirchner, J. W.: Catchments as simple dynamical systems: Catchment characterization, rainfall-runoff modeling, and doing hydrology backward, Water Resour. Res., 45, W02429, doi:10.1029/2008WR006912, 2009.

Klemm, O., and Wrzesinski, T.: Fog deposition fluxes of water and ions to a mountainous site in Central Europe, Tellus 59, 705-714, 2007.

Kling, H.: Spatio-temporal modelling of the water balance of Austria. Dissertation, University of Natural Resources and Applied Life Sciences, 234 pp., available at: http://iwhw.boku.ac.at/dissertationen/kling.pdf (last access: 7 October 2014), 2006.

Kling, H., and Nachtnebel, H.P.: A method for the regional estimation of runoff separation parameters for hydrological modelling, J. Hydrol., 364, 163–174, 2009.

Kling, H., Stanzel, P., Fuchs, M., and Nachtnebel, H.P.: Performance of the COSERO precipitation-runoff model under non-stationary conditions in basins with different climates, Hydrolog. Sci. J., doi: 10.1080/02626667.2014.959956, in press, 2015.

Krajewski, W.F., and Smith, J.A.: Radar hydrology: rainfall estimation, Adv. Water Resour., 25, 1387-13, 2002.

Krajewski, W.F., Villarini, G., and Smith, J.A.: RADAR-rainfall uncertainties, B. Am. Meteorol. Soc., 91, 87–94. doi:10.1175/2009BAMS2747.1, 2010

Krier, R., Matgen, P., Goergen, K., Pfister, L., Hoffmann, L., Kirchner, J. W., Uhlenbrook, S., and Savenije, H.H.G.: Inferring catchment precipitation by doing hydrology backward: A test in 24 small and mesoscale catchments in Luxembourg, Water Resour. Res., 48, W10525, doi:10.1029/2011WR010657, 2012.

Kuczera, G., Kavetski, D., Franks, S., and Thyer, M.: Towards a Bayesian total error analysis of conceptual rainfall-runoff models: Characterising model error using storm-dependent parameters, J. Hydrol., 331, 161–177, 2006.

Kunstmann, H., and Stadler, C.: High resolution distributed atmospheric-hydrological modeling for Alpine catchments, J. Hydrol., 314, 105-124, 2005.

Liu, Y., Weerts, A. H., Clark, M., Hendricks Franssen, H.-J., Kumar, S., Moradkhani, H., Seo, D.-J., Schwanenberg, D., Smith, P., van Dijk, A. I. J. M., van Velzen, N., He, M., Lee, H., Noh, S. J., Rakovec, O., and Restrepo, P.: Advancing data assimilation in operational hydrologic forecasting: progresses, challenges, and emerging opportunities. Hydrol. Earth Syst. Sci., 16, 3863-3887, 2012.

McLaughlin, D.: An integrated approach to hydrologic data assimilation: interpolation, smoothing and filtering. Advances in Water Resources, 25, 1275-1286, 2002.

McMillan, H., Freer, J., Pappenberger, F., Krueger, T., and Clark, M.: Impacts of uncertain river flow data on rainfall-runoff model calibration and discharge predictions, Hydrol. Process., 24, 1270–1284, doi:10.1002/Hyp.7587, 2010.

Nachtnebel, H. P., Herrnegger, M., Kahl, B., and Hepp, G.: Meteorologisch-hydrologisches Warnsystem Steyr: Endbericht und Technische Dokumentation - Teil 3 - Hydrologische Abflussmodellierung, Amt der OÖ Landesregierung - Abteilung Wasserwirtschaft, Schutzwasserwirtschaft und Hydrographie, 197, 2010a.

Nachtnebel, H.P., Senoner, T., Kahl, B., Apperl, B., and Waldhör, B.: Hochwasserprognosesystem Ybbs - Hydrologische Abflussmodellierung, Amt der NÖ Landesregierung, St. Pölten, 176, 2010b.

Nachtnebel, H.P., Haberl, U., Stanzel, Ph., Kahl, B., Holzmann, H., and Pfaffenwimmer, Th.: Hydrologische Abflussmodellierung - Teil 3, in: Amt der Salzburger Landesregierung: HydrisII Hydrologisches Informationssystem zur Hochwasservorhersage im Land Salzburg, Amt der Salzburger Landesregierung, 341, 2009a.

Nachtnebel, H. P., Senoner, T., Stanzel, P., Kahl, B., Hernegger, M., Haberl, U. and Pfaffenwimmer, T.: Inflow prediction system for the Hydropower Plant Gabčíkovo, Part 3 - Hydrologic Modelling, Slovenské elektrárne, a.s. Bratislava, 139, 2009b.

Nachtnebel, H.P., Baumung, S., and Lettl, W.: Abflussprognosemodell für das Einzugsgebiet der Enns und Steyr, report, Institute of Water Management, Hydology and Hydraulic Engineering, University of Natural Resources and Applied Life Sciences, Vienna, Austria, 1993.

Nash, J. E., and Sutcliffe, J. V.: River flow forecasting through conceptual models, Part I: A discussion of principles, J. Hydrol., 10, 282–290, 1970.

Pappenberger, F., Matgen, P., Beven, K.J., Henry J.B., Pfister, L., and de Fraipont, P.: Influence of uncertain boundary conditions and model structure on flood inundation predictions, Adv. Water Resour., 29, 1430–1449, 2006.

Pelletier, M.P.: Uncertainties in the determination of river discharge: a literature review, Can. J. Civ. Eng., 15, 834–850, 1987.

Perrin, C., Michel, C., and Andréassian, V.: Does a large number of parameters enhance model performance? Comparative assessment of common catchment model structures on 429 catchments, J. Hydrol., 242, 275–301, 2001.

Press, W.H., Teukolsky, S.A., Vetterling, W.T., and Flannery, B.P.: Numerical Recipes in FORTRAN, The Art of Scientific Computing, Cambridge Univ. Press, New York, 965 pp., 1992.

Seibert, J.: Reliability of model predictions outside calibration conditions, Nord. Hydrol., 34, 477–492, 2003.

Seibert, J., and Morén, A.-S.: Reducing systematic errors in rainfall measurements using a new type of gauge, Agric. Forest. Meteorol., 98–99, 341–348, 1999.

Sevruk, B.: Methodische Untersuchungen des systematischen Messfehlers der Hellmann-Regenmesser im Sommerhalbjahr in der Schweiz, Dissertation, Eidgenöss. Techn. Hochsch. Zürich, Zürich, Switzerland, 1981.

Sevruk, B.: Correction of precipitation measurements. Proc. Workshop on the Correction of Precipitation Measurements, in: Zürcher Geographische Schriften, ETH Zürich, p. 289, 1986.

Sevruk, B., and Nespor, V.: Empirical and theoretical assessment of the wind induced error of rain measurement, Water Sci. Technol., 37, 171–178, 1998.

Simoni, S., Padoan, S., Nadeau, D.F., Diebold, M., Porporato, A., Barrenetxea, G., Ingelrest, F., Vetterli, and M., Parlange, M.B.: Hydrologic response of an alpine watershed: application of a meteorological wireless sensor network to understand streamflow generation, Water Resour. Res., 47, W10524, doi:10.1029/2011WR010730, 2011.

Stanzel, Ph., Kahl, B., Haberl, U., Herrnegger, M., and Nachtnebel, H. P.: Continuous hydrological modeling in the context of real time flood forecasting in alpine Danube tributary catchments, IOP Conference Series, 4, 012005, doi:10.1088/1755-1307/4/1/01200, 2008.

Sugawara, M.: On the weights of precipitation stations. in: O’Kane, J.P. (Ed.), Advances in Theoretical Hydrology, edited by O´Kane, J.P., Elsevier Science Publishers, Amsterdam, 59–74, 1992.

Tarantola, A.: Inverse problem theory and methods for model parameter estimation, Society for Industrial and Applied Mathematics, Philadelphia, 352 pp., 2005.

Valéry, A., Andréassian, V., and Perrin, C.: Inverting the hydrological cycle: when streamflow measurements help assess altitudinal precipitation gradients in mountain areas, in: New Approaches to Hydrological Prediction in Data–sparse Regions, IAHS Publ., 333, 281-286, 2009.

Valéry, A., Andréassian, V., and Perrin, C.: Regionalisation of rainfall and air temperature over high-altitude catchments – learning from outliers, Hydrol. Sci. J., 55, 928–940, 2010.

van Genuchten, M. T.: A closed-form equation for predicting the hydraulic conductivity of unsaturated soils, Soil Sci. Soc. Am J., 44, 892-898, 1980.

Vrugt, J.A., ter Braak, C.J.F., Clark, M.P., Hyman, J.M., and Robinson B.A.: Treatment of input uncertainty in hydrologic modeling: doing hydrology backward with Markov chain Monte Carlo simulation, Water Resour. Res., 44, W00B09, doi:10.1029/2007WR006720, 2008.

Wood, S.J., Jones, D.A., and Moore, R.J.: Accuracy of rainfall measurement for scales of hydrological interest, Hydrol. Earth Syst. Sci., 4, 531–543, doi:10.5194/hess-4-531-2000.

Tables

Table 1: Magnitude of different systematic errors in precipitation measurements (Sevruk, 1981, 1986; Goodison et al, 1998; Elias et al., 1993; Jacobs et al., 2006; Klemm and Wrzesinsky, 2007).

Systematic error	Magnitude
Wind-induced errors	2 - 10 % (liquid precipitation) 10 - >50 % (snow)
Wetting losses	2 - 10 %
Evaporation losses	0 - 4 %
Splash-out and splash-in	1 - 2 %
Flog and dew	4 - 10 %

Table 2: Model parameters θ_i. Parameters in *italics* are calibrated.

Parameter	Units	Range	Description
INTMAX	mm	0.5 - 2.5	Interception storage capacity
M	mm	80 - 250	Soil storage capacity
FKFAK	-	0.5 - 1	Critical soil moisture for actual evapotranspiration
ETVEGCOR	-	0.4 - 1.1	Vegetation correction factor for actual evapotranspiration from soil
BETA	-	0.1 - 10	Exponent for computing fast runoff generation
KBF	h	4000 - 12000	Recession coefficient for percolation from soil module
PEX2	-	5 - 25	Parameter for non-linear percolation
TAB2	h	50 - 500	Recession coefficient for interflow
TVS2	h	50 - 500	Recession coefficient for percolation from interflow reservoir
H2	mm	0 - 25	Outlet height for interflow
TAB3	h	1000 - 5000	Recession coefficient for base flow
TAB4	h	0.05 - 10	Recession coefficient for routing

Table 3: Model fluxes and system states S_i. Fluxes represent sums over the time step.

Variable	Units	Type	Description
R	mm	Input	Rainfall
ETp	mm	Input	Potential evapotranspiration
ETI	mm	Output	Actual Evapotranspiration from interception module
ETG	mm	Output	Actual Evapotranspiration from soil module
BWI	mm	State	Water stored in interception module
BW0	mm	State	Water stored in soil module
BW2	mm	State	Water stored in interflow reservoir
BW3	mm	State	Water stored in base flow reservoir
BW4	mm	State	Water stored in routing reservoir
R_Soil	mm	Internal flux	Input into soil module
Q1	mm	Internal flux	Fast runoff from soil module
Q2	mm	Internal flux	Percolation from soil module
QAB2	mm	Internal flux	Interflow
QVS2	mm	Internal flux	Percolation from interflow reservoir
QAB3	mm	Internal flux	Base flow
QSIM	mm	Output	Total runoff

Table 4: Characteristics of the study catchments (BMLFUW, 2007; BMLFUW, 2009).

	Schliefau	Krems
Basin area [km²]	17.9	38.4
Mean elevation [m]	608	598
Elevation range [m]	390 - 818	413 - 1511
Mean annual precipitation [mm]	1390	1345
Mean annual runoff [m³/s]	0.38	1.12

Table 5: Overview of the model calibration and simulations experiments with observed input data. PObs and PInca refer to the rainfall from the station observations and the INCA system.

	Jun. to Sept. in year				Driving input (Forward / inverse model)	Purpose
	2006	2007	2008	2009		
Exp1	calib.	valid.	valid.	valid.	PObs / Q	Influence of different calibration periods on simulations
Exp2	calib.	calib.	valid.	valid.	PObs / Q	
Exp3	calib.	calib.	calib.	valid.	PObs / Q	
Exp4	calib.	calib.	calib.	valid.	PObs / Q+10%	Influence of different runoff Q on simulations
Exp5	calib.	calib.	calib.	valid.	PInca / Q	Influence of different rainfall input on simulations
Exp6	Parameters from Exp3, but different initial conditions				PObs / Q	Influence of cold states on simulations

Table 6: Model performance for the different simulation experiments and the two catchments of the forward model, expressed by Nash-Sutcliffe-Efficiency (NSE) and the mean bias between simulated and observed runoff in percent of observed runoff for the period 2006 to 2009. Only the months June to September are evaluated.

		NSE [-]	mean BIAS [%]
Schliefau	Exp1	0.822	7.8
	Exp2	0.832	3.9
	Exp3	0.828	0.9
	Exp4	0.830	-5.9
	Exp5	0.728	-0.6
Krems	Exp1	0.763	-1.4
	Exp2	0.851	-4.8
	Exp3	0.851	-4.8
	Exp4	0.854	-7.9
	Exp5	0.787	1.5

Table 7: Correlation for 2006 to 2009 between different rainfall realisations and temporal aggregation lengths. (PObs: Ground observation, PInv: Inverse rainfall from Exp1 to Exp5, PInca: INCA rainfall).

		CORR: 1h-sums			CORR: 6h-sums			CORR: 24h-sums		
		PObs - PInv	PInca - PInv	PObs - PInca	PObs - PInv	PInca - PInv	PObs - PInca	PObs - Pinv	PInca - PInv	PObs - PInca
Schliefau	Exp1	0.504	0.251		0.800	0.671		0.871	0.802	
	Exp2	0.549	0.290		0.828	0.703		0.914	0.840	
	Exp3	0.534	0.284	0.463	0.824	0.699	0.849	0.918	0.845	0.928
	Exp4	0.530	0.283		0.818	0.695		0.917	0.843	
	Exp5	0.524	0.276		0.824	0.697		0.920	0.842	
Krems	Exp1	0.478	0.394		0.794	0.771		0.871	0.847	
	Exp2	0.517	0.445		0.831	0.807		0.909	0.889	
	Exp3	0.517	0.445	0.469	0.831	0.807	0.864	0.909	0.889	0.931
	Exp4	0.517	0.445		0.833	0.809		0.909	0.892	
	Exp5	0.503	0.445		0.820	0.805		0.901	0.888	

Table 8: Mean Bias for 2006 to 2009 between different rainfall realisations.

		Mean Bias [mm/d]	
		PInv - PObs	PInca - PObs
Schliefau	Exp1	0.14	
	Exp2	0.07	
	Exp3	0.22	0.02
	Exp4	0.42	
	Exp5	0.33	
Krems	Exp1	0.28	
	Exp2	0.40	
	Exp3	0.40	0.47
	Exp4	0.53	
	Exp5	0.49	

Figures

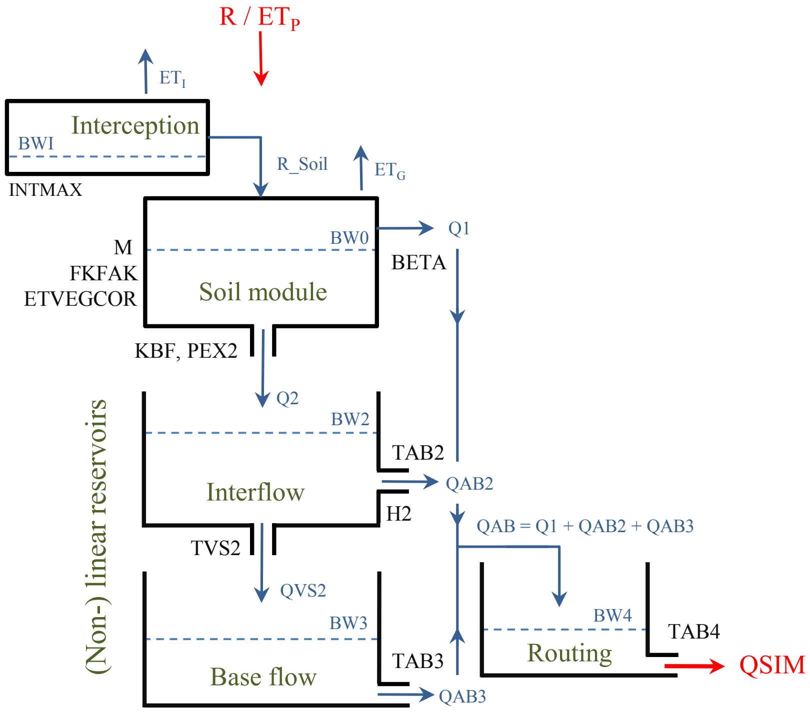

Figure 1: Structure, parameters and states of the forward model.

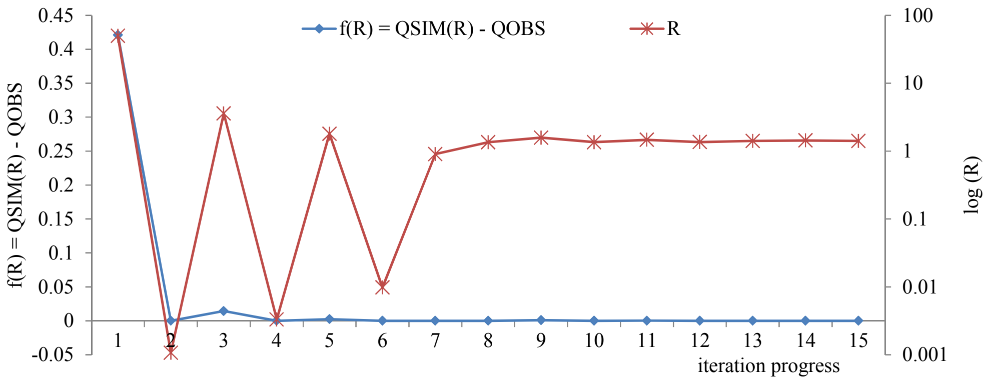

Figure 2: Illustration of the iteration progress for one model time step. Note that the right y-axis showing the inverse rainfall values (R) is in a logarithmic scale.

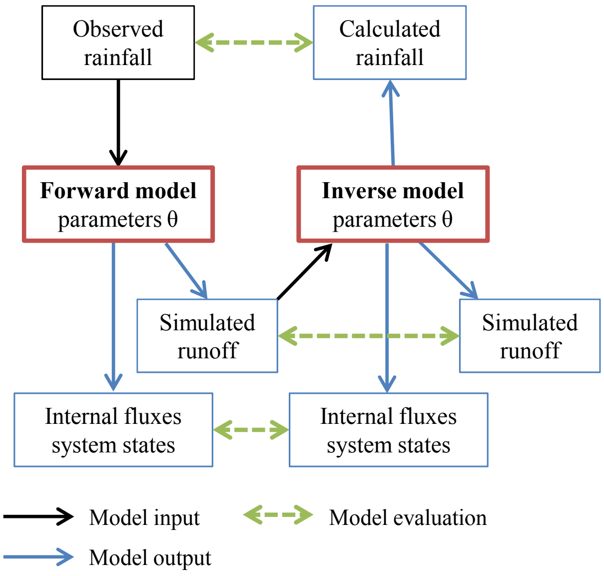

Figure 3: Setup of the virtual experiments and evaluation of the inverse model. All variables are calculated for every Monte Carlo run, in which parameters θ are varied.

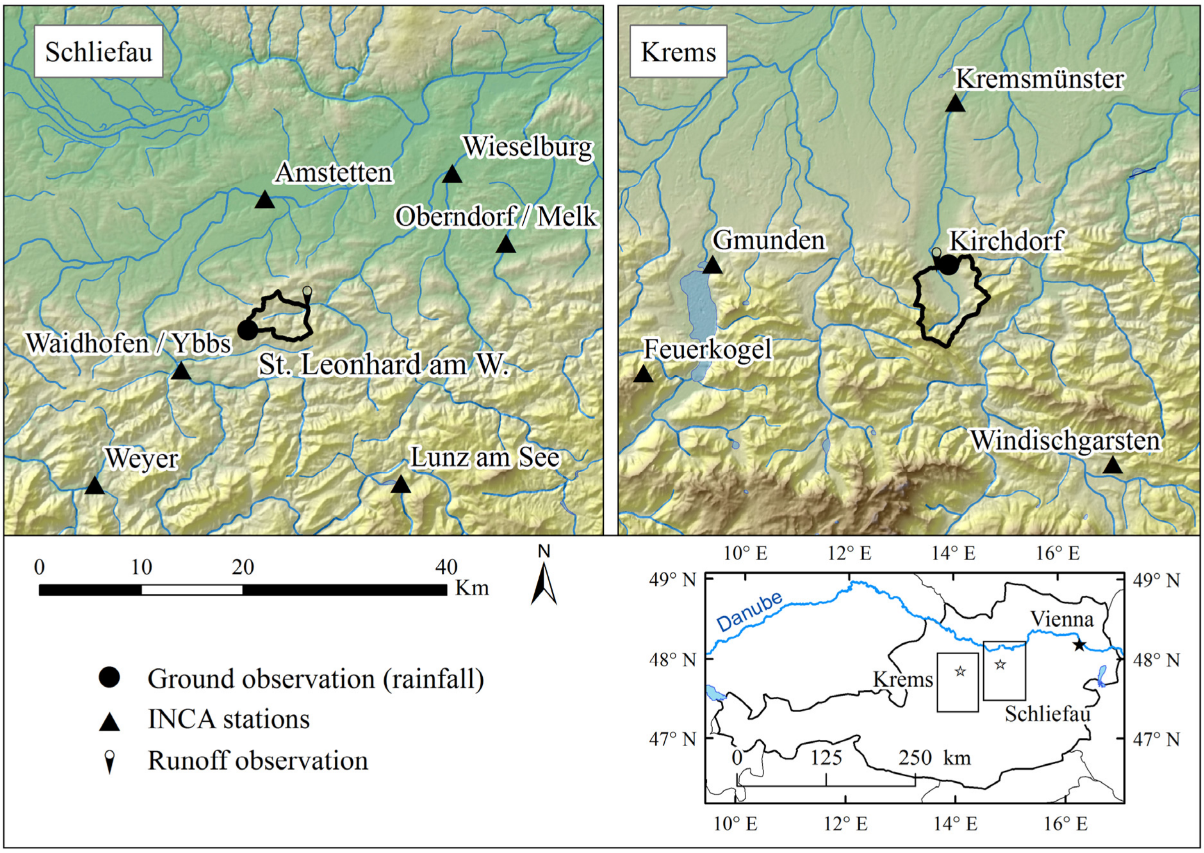

Figure 4: Schliefau and Krems catchment and location of meteorological stations. Note that ground observation of rainfall is not part of the INCA stations network.

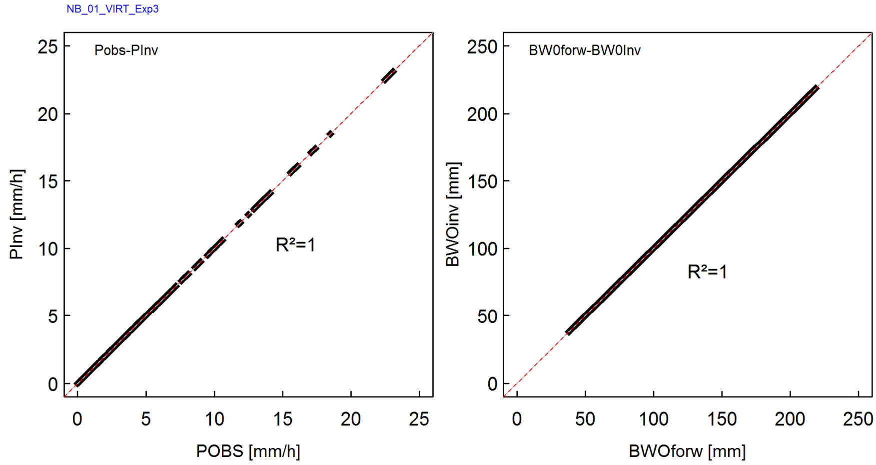

Figure 5: Virtual experiment with simulated runoff as input into the inverse model (Schliefau catchment): Identical observed and inverse rainfall (POBS-PInv, left) and soil water content of forward and inverse model (BW0forw-BW0Inv, right).

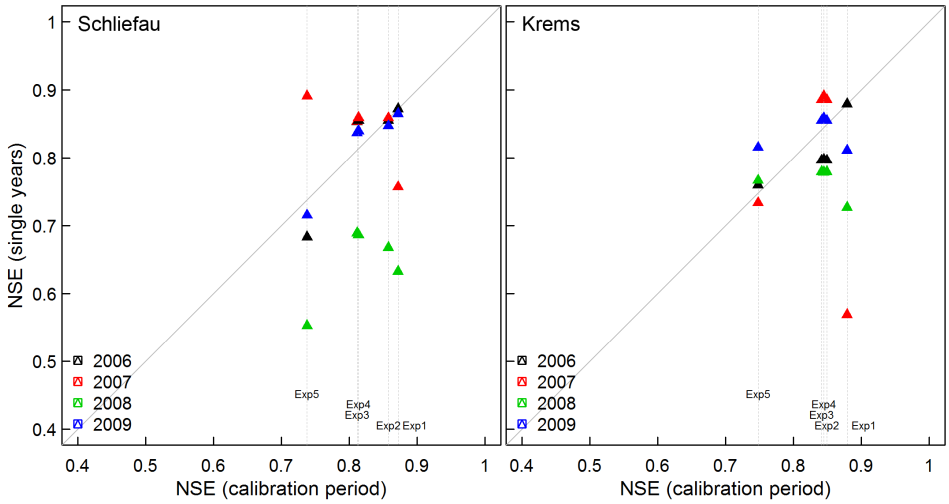

Figure 6: Nash-Sutcliffe-Efficiency (NSE) of the forward model for the calibration periods versus single years for the 2 study areas.

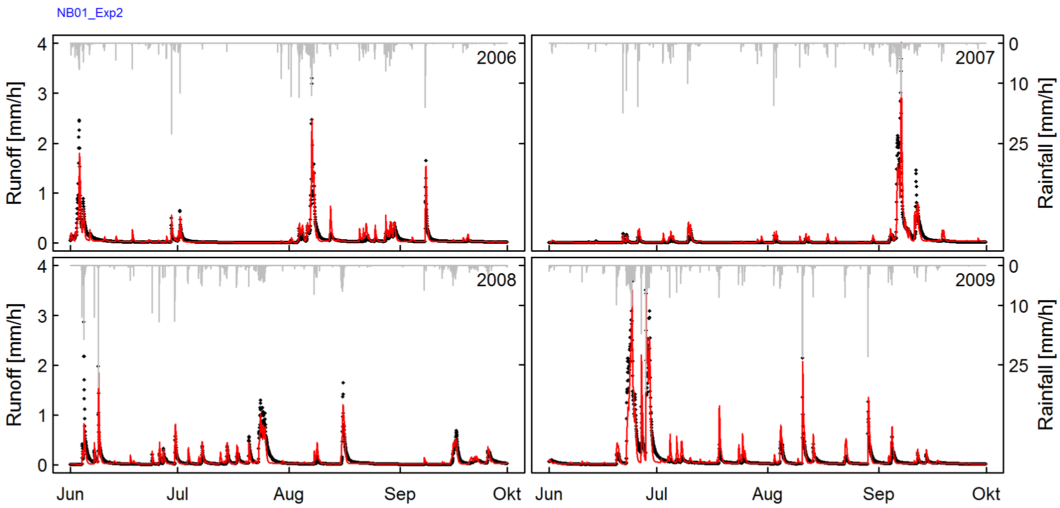

Figure 7: Schliefau catchment: Observed (black points) and simulated (red) runoff of Exp2.

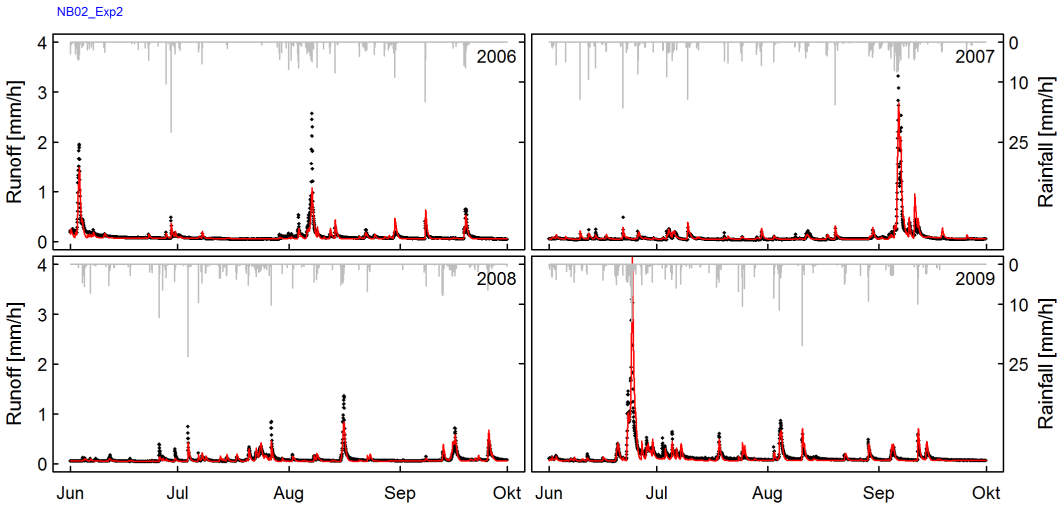

Figure 8: Krems catchment: Observed (black points) and simulated (red) runoff of Exp2.

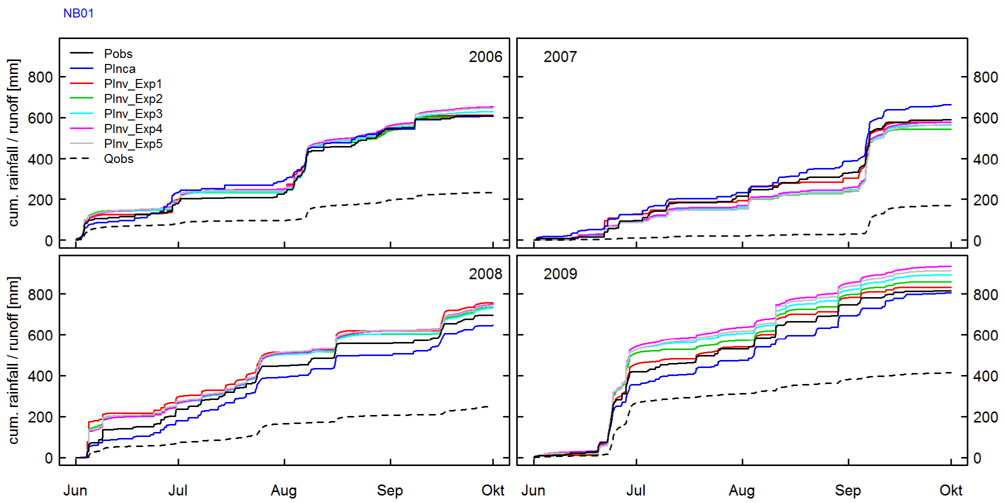

Figure 9: Schliefau catchment: Cumulative rainfall curves for observed rainfall (PObs), INCA rainfall (PInca) and the inverse rainfall of Exp1 to Exp5 (PInv). Cumulative sums of observed runoff are shown as dashed black lines.

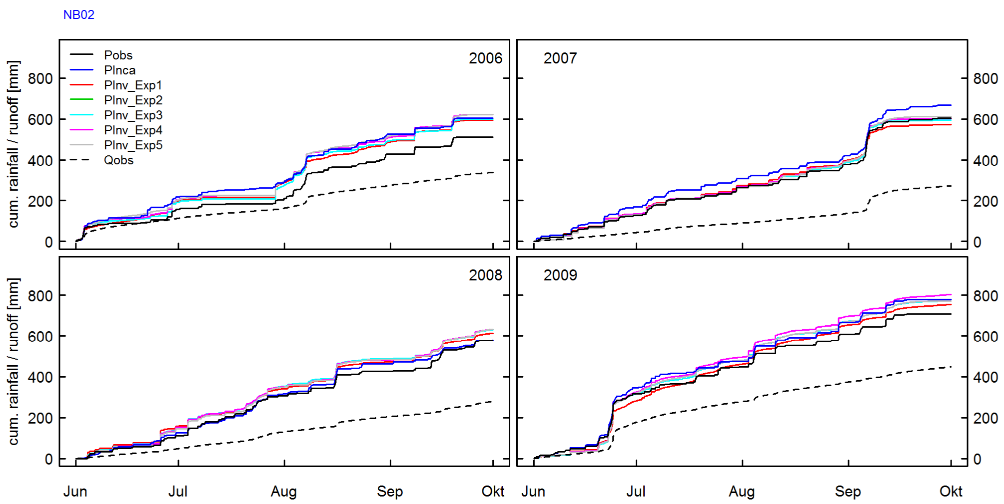

Figure 10: Krems catchment: Cumulative rainfall curves for observed rainfall (PObs), INCA rainfall (PInca) and the inverse rainfall of Exp1 to Exp5. Cumulative sums of observed runoff are shown as dotted black lines.

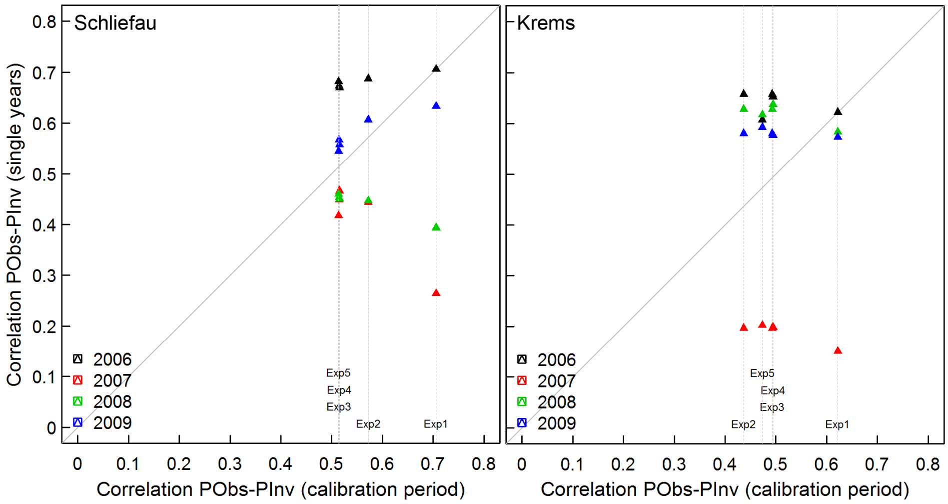

Figure 11: Correlation between PObs-PInv for the calibration periods of the simulation experiments Exp1 to Exp5 versus single years for the 2 study areas.

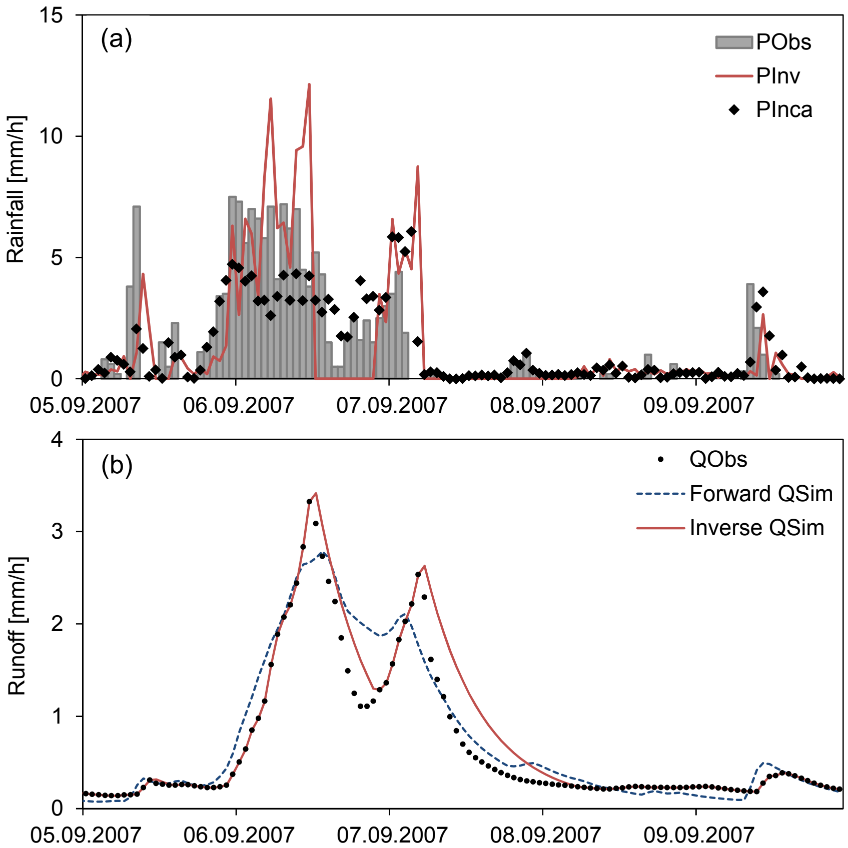

Figure 12: Krems catchment: Temporal development of the different rainfall realisations (a) and runoff (b) for a flood event. Simulations originate from Exp3.

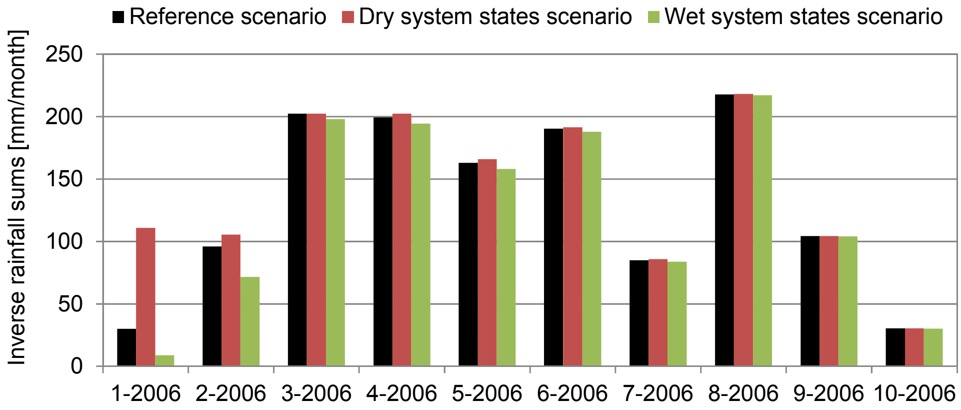

Figure 13: Krems catchment: Monthly sums of inverse rainfall simulated in the scenarios "reference", "dry" and "wet" from Exp6.